



## Effects of reflective and luminosity behaviours on locations of triangular Lagrangian points in the Satellite -Proxima Centauri system with capricious masses

\*<sup>1</sup>Cyril-Okeme, V., <sup>2</sup>Zubairu, K., <sup>2</sup>Mbaskabkwe, L., & <sup>3</sup>Oni, L.

<sup>1</sup>Department of Mathematics, Faculty of Physical Sciences, Federal University, Lokoja, Kogi-State Nigeria

<sup>2</sup>Department of Mathematics, Faculty of Science Education, Federal University of Education, Zaria, Kaduna-State

<sup>3</sup>Department of Mathematics, College of Physical Science, Joseph Sarwuan Tarka University, Nigeria

\*Corresponding author email: [veronica.cyril-okeme@fulokoja.edu.ng](mailto:veronica.cyril-okeme@fulokoja.edu.ng).

### Abstract

This investigation unveils effects of reflective and luminosity tendencies of a binary star, Proxima Centauri on locations of the triangular Lagrangian points (TLPs) when Proxima is a radiating star and Centauri, though also radiating but possesses reflective mode. The masses and luminosities of the stars are assumed to change with time within the confines of the unified Meshchersky law and their dynamical frameworks are guided by the Gylden-Meshchersky model. We deduced the equations of motion and obtained the TLPs of both the time-variant and the time-invariant systems. It is observed that the locations and zero velocity curves are influenced by the reflective and luminous effects of the stars. This investigation enhances our understanding of the multifaceted gravitational and radiative forces in variable mass celestial systems, and are relevant in space missions where a satellite is launched in the gravitational environment of binary systems having a radiating and reflective behaviors with capricious masses.

**Keywords:** R3BP, Capricious Masses, Proxima Centauri, Luminosity, Reflective System.

### Introduction

The conventional form of the restricted three-body problem (RTBP) as studied by Szebehely (1967) is one of the most studied models in celestial mechanics. This formulation describes dynamics of a test particle of negligible mass which moves under the impact of gravity of two massive bodies that revolve in circular paths about their mutual centre of mass and the test particle not influencing the motion of the bodies. Five solutions are known and are called the liberation, Lagrangian points (LPs) or equilibrium points. Two of these solutions forms triangles with the two bodies and are termed triangular Lagrangian points (TLPs), while three are located on the line connecting the two bodies and are referred to as collinear Lagrangian points (CLPs). These points have numerous applications in space missions such as station parking, an nearby Earth orbits and satellite constellations (Szebehely 1967).

An important extension of the classical RTBP is the photogravitational formulation, where one or both the two bodies are emitters of radiation pressure. AbdulRaheem & Singh (2006) investigated the collective effect of perturbations, radiation and oblateness on the positions and stability of the LPs in the RTBP while, Singh and Leke (2010) studied the photogravitational RTBP with capricious masses by taking both main bodies as radiation emitters. Another extension of the RTBP is the inclusion of the albedo or reflective effect, which represents the fraction of radiation reflected by the smaller body. In contrast to the classical RTBP of Szebehely (1967) that assumes a perfectly absorbing smaller primary, in real celestial bodies reflection of a part of the incoming radiation, is common phenomenon and it alters the system's dynamics.

The first study of effects of reflection on positions and stability of the LPs was studied by Idrisi (2017) where they analyzed the albedo-modified problem and showed that reflected radiation can significantly shift the LPs, especially

the TLPs, while the numerical and graphical positions of non-collinear LPs, considering the albedo effect and oblateness of the smaller body, were carried out by Idrisi &Ullah (2018). Yadav et al. (2021) explored the stabilization of LPs in the Sun–Jupiter system with a non-ideal solar sail and impact of albedo, while, Jat and Kishor (2025) showed that inclusion of both the reflective ability and dark matter halo effects is essential when modeling out-of-plane motion. In general, all these studies establish reflected radiation as a critical factor for genuine and precise modeling of celestial dynamics.

Finally, the classical model of the RTBP did not consider the aspect where the masses of the bodies change with time. However, due to isotropic radiation in space, scientists formulated the RTBP with capricious masses. Several of these scientists and researchers, Bekov (1988), Luk’yanov (1989), Singh and Leke (2010, 2012, 2013), Gao and Wang (2020), Abouelmagd et al. (2021), Leke and Singh (2023), Leke and Mmaju (2023), and more recently, Leke and Orum (2024), Putra et al. (2024), Leke et al. (2024, 2025a), Leke and Akpii (2025), Leke et al. (2025b) and Cyril-Okeme et al. (2025), amongst others.

Inspired by the research of Singh and Leke (2010) and the numerous astrophysical implications of the RTBP with capricious masses, we thought it reasonable to examine the effects of reflective and luminosity behaviours of Proxima-Centauri on locations of TLPs by following the methodology of Idrisi (2017) with further assumptions that the luminosities of the stars are not constant but change with time by the unified Meshchersky law (UML) while the movements of the stars is guided by the Gylden-Meshchersky problem (GMP). The idea of infusing variable luminosities and albedo in the RTBP is that the model provides a robust and more precise illustration of the real-world motion of celestial bodies and permits for enhanced dynamical estimates of their impending behaviours.

By introducing the luminosity parameter  $\kappa_1$ , which represents the ratio of the luminosities of the smaller star to the larger star, with very small value of  $\kappa_1$  corresponds to low reflective character of the smaller star while values of  $\kappa_1$  close to a unit indicates an almost equal luminosities or a high reflective tendency of the smaller star. This paper aims to understand how this parameter influences the locations, of a satellite in the TLPs. The paper is structured in the following set up as follows: in section 2, the equations of motion are given while in Section 3, we calculate the positions of the TLPs and the numerical applications, while Sections 4 and contain the discussion and conclusion, respectively.

### Equations of Motion

We begin the procedure of the derivations of the equations of motion of the two-body problem (2BP), which is the preparatory set up for almost all reference books in the area of astrodynamics. The 2BP defines the motion of two masses under their mutual gravitational attraction, and is given by

$$\frac{d\vec{v}}{dt} = -\frac{\mu}{r^2} \frac{\vec{r}}{r} \quad (1)$$

where  $\vec{v}$  is the velocity,  $\mu$  is the product of the gravitational constant  $G$  and the sum of the masses, and  $\vec{r}$  is the distance between the bodies and connects the angular velocity  $\theta$  and constant of the area integral  $C$  by the relation:

$$r^2 \dot{\theta} = C \quad (2)$$

Therefore, the GMP of a both radiating star with variable masses, is such that

$$\ddot{\vec{r}} = -G \frac{(m_1 q_1 + m_2 q_A)}{r^3} \vec{r} \quad (3)$$

where  $q_1$  is the radiation factor of the larger star and  $q_A$  is the reflective effect of the smaller one, while  $G$  is the gravitational constant.

Next, following Singh and Leke (2010), we adopt a synodic coordinate system  $Oxyz$ , where  $O$  is the origin. Let  $m_1$  and  $m_2$  be the masses of the larger and smaller star, respectively, while  $m_3$  is the mass of the satellite. The  $x$  –axis is taken to be the line joining the stars and the coordinates of  $m_1$  and  $m_2$  are  $(x_1, 0, 0)$  and  $(x_2, 0, 0)$  respectively, while that of the satellite is  $(x, y, z)$ . Let the distances of  $m_3$  to  $m_1$  and  $m_2$  be  $r_1$  and  $r_2$ , respectively, while the distance between the stars is  $r$  and  $\omega$  is the angular velocity, as shown in Fig 1.

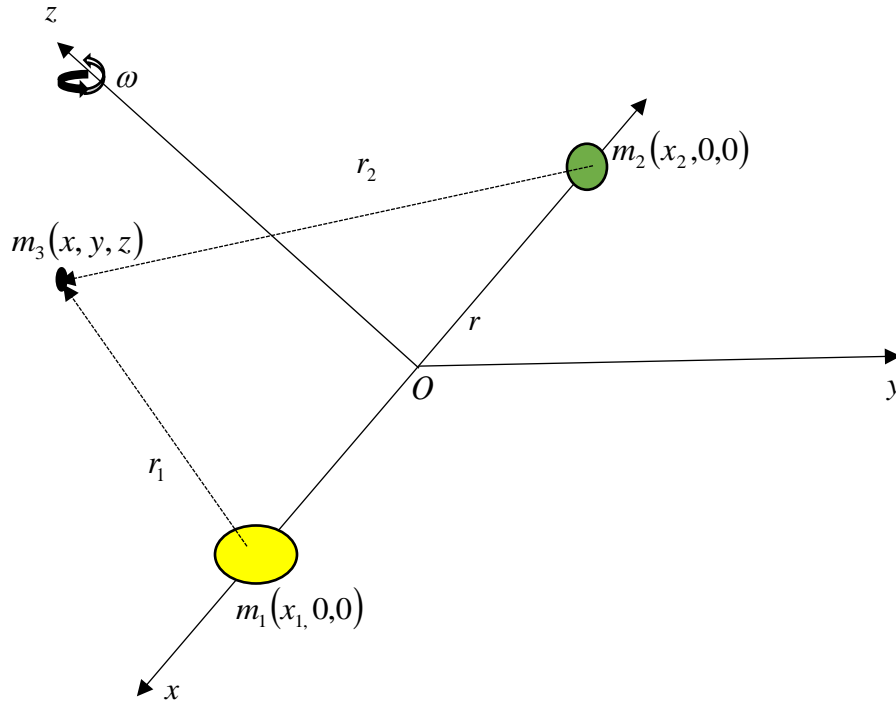


Fig 1: Configuration of the Model

Now, the kinetic energy of a satellite in the barycentric frame of reference  $Oxyz$  is given by

$$T = \frac{1}{2}m_3(\dot{x}^2 + \dot{y}^2 + \dot{z}^2) + m_3\omega(x\dot{y} - y\dot{x}) + \frac{1}{2}m_3(x^2 + y^2)\omega^2 \quad (4)$$

while its potential energy, when the masses of the stars change with time is:

$$U = -Gm_3 \left[ \frac{m_1(t)q_1}{r_1} + \frac{m_2(t)q_A}{r_2} \right] \quad (5)$$

where  $r_1^2 = (x - x_1)^2 + y^2 + z^2$ ,  $r_2^2 = (x - x_2)^2 + y^2 + z^2$

The equation that connects the reflective tendency and radiation pressure is (Idrisi 2017; Idrisi & Ullah 2018)

$$q_1 = 1 - (1 - q_A) \frac{m_2 L_{b1}}{m_1 L_{b2}} \quad (6)$$

where  $L_{b1}$  and  $L_{b2}$  are the luminosity of the larger and the smaller stars, respectively and are assumed to change with time as the masses of the stars alter with time.

Therefore, adopting the methods used in Singh & Leke (2010), the dynamical equations of a passively gravitating satellite in the fields of the stars are obtained:

$$\ddot{x} - 2\omega\dot{y} = \omega^2 x + \dot{\omega}y - \frac{\mu_1 q_1 (x - x_1)}{r_1^3} - \frac{\mu_2 q_A (x - x_2)}{r_2^3}$$

$$\ddot{y} + 2\omega\dot{x} = \omega^2 y - \dot{\omega}x - \frac{\mu_1 q_1 y}{r_1^3} - \frac{\mu_2 q_A y}{r_2^3} \quad (7)$$

$$\ddot{z} = -\frac{\mu_1 q_1 z}{r_1^3} - \frac{\mu_2 q_A z}{r_2^3}$$

where

$$\omega^2(t) = \frac{1}{r^3} \frac{\mu(t)}{\kappa}, \mu_1(t) = Gm_1(t), \mu_2(t) = Gm_2(t), \mu(t) = Gm_1(t) + Gm_2(t) \quad (8)$$

and  $\kappa$  is a constant of the particular integral

$$r\mu = \kappa C^2, \quad (9)$$

of the GMP.

Equations (7-8) describe the time-variant motion of a satellite under the gravitational influence of the stars when both stars' experience mass variations while the larger star is a radiation emitter and the smaller one reflects a portion of the incident radiation.

Next, because the equations (7-8) are non-integrable time-variant differential equations with variable coefficients, we suppose that the luminosities and radii of the bodies alter with time as defined by the UML:

$$L_{b1} = L_{01}R^2(t), L_{b2} = L_{02}R^2(t) \text{ and } R_{1,2}^* = \rho_{1,2}^*R(t) \quad (10)$$

Hence, equation (6) is cast to the form

$$1 - q_1 = (1 - q_A) \frac{\mu_{20} L_{01}}{\mu_{10} L_{02}} \quad (11)$$

which consequently reduces to

$$q_1 = 1 - \frac{v\alpha_A}{(1-v)k_1} \quad (12)$$

where  $\alpha_A = 1 - q_A$ ,  $k_1 = \frac{L_{02}}{L_{01}}$  is a constant and is such that  $k_1 \in (0,1)$  while  $0 < q_1 \leq 1$  and  $q_1 \leq \alpha_A$  where  $\alpha_A \ll 1$

Hence, the autotomized equations corresponding to (7-8) after choosing units of measurements and substituting equation (12), yields

$$\xi'' - 2\eta' = \frac{\partial\Omega}{\partial\xi}, \quad \eta'' + 2\xi' = \frac{\partial\Omega}{\partial\eta}, \quad \zeta'' = \frac{\partial\Omega}{\partial\zeta} \quad (13)$$

where

$$\Omega = \frac{\kappa}{2}(\xi^2 + \eta^2 + \zeta^2) - \frac{\zeta^2}{2} + \frac{\kappa[k_1(1-v) - v\alpha_A]}{k_1\rho_1} + \frac{\kappa(1-\alpha_A)v}{\rho_2} \quad (14)$$

$$\rho_1 = \sqrt{(\xi + v)^2 + \eta^2 + \zeta^2}, \rho_2 = \sqrt{(\xi + v - 1)^2 + \eta^2 + \zeta^2} \quad (15)$$

When  $\kappa = 1$ , and  $\zeta = 0$ , the equations (13-16) fully coincide with those of Idrisi (2017) and differ from those of Singh & Leke (2010) due to the luminosity parameter  $k_1$

Eqs (13) have the Jacobi integral

$$2\Omega(\xi, \eta, \zeta, \kappa, v, q_A, ) - U = J \quad (16)$$

where

$$U = \sqrt{\xi'^2 + \eta'^2 + \zeta'^2}$$

and J is the Jacobi constant.

### Locations of Triangular Points

The TLPs are the solutions of equations (13) when  $\zeta = 0$ . On this ground, the system of Eqs (13) reduce to

$$\xi'' - 2\eta' = \frac{\partial\Omega}{\partial\xi}, \quad \eta'' + 2\xi' = \frac{\partial\Omega}{\partial\eta}, \quad \zeta'' = \frac{\partial\Omega}{\partial\zeta} \quad (17)$$

where

$$\Omega = \frac{\kappa}{2}(\xi^2 + \eta^2) + \frac{\kappa[k_1(1-v) - v\alpha_A]}{k_1\rho_1} + \frac{\kappa(1-\alpha_A)v}{\rho_2} \quad (18)$$

where

$$\rho_1 = \sqrt{(\xi + v)^2 + \eta^2}, \rho_2 = \sqrt{(\xi + v - 1)^2 + \eta^2}, \quad (19)$$

To obtain the TLPs we equate the components of the velocity and acceleration to zero in equation (17), to get

$$\kappa\xi - \frac{\kappa[k_1(1-v) - v\alpha_A](\xi + v)}{k_1\rho_1^3} - \frac{\kappa(1-\alpha_A)v(\xi + v - 1)}{\rho_2^3} = 0 \quad (20)$$

and

$$\kappa\eta - \frac{\kappa\kappa[k_1(1-v)-v\alpha_A]\eta}{k_1\rho_1^3} - \frac{\kappa(1-\alpha_A)v\eta}{\rho_2^3} = 0 \quad (21)$$

Since  $\kappa\eta \neq 0$  and  $\eta \neq 0$ , equations (20) and (21) become

$$\xi - \frac{[k_1(1-v)-v\alpha_A](\xi+v)}{k_1\rho_1^3} - \frac{(1-\alpha_A)v(\xi+v-1)}{\rho_2^3} = 0 \quad (22)$$

and

$$1 - \frac{[k_1(1-v)-v\alpha_A]}{k_1\rho_1^3} - \frac{(1-\alpha_A)v}{\rho_2^3} = 0 \quad (23)$$

Next, multiply equation (23), by  $\xi + v$ , to get

$$(\xi + v) - \frac{[k_1(1-v)-v\alpha_A](\xi+v)}{k_1\rho_1^3} - \frac{(1-\alpha_A)v(\xi+v)}{\rho_2^3} = 0 \quad (24)$$

Subtract (24) from (22), to get

$$v \left[ 1 - \frac{(1-\alpha_A)}{\rho_2^3} \right] = 0$$

But  $v \neq 0$ , therefore, we have

$$\rho_2^3 = (1 - \alpha_A) \quad (25)$$

Similarly, we get

$$\rho_1^3 = \frac{[k_1(1-v)-v\alpha_A]}{k_1(1-v)} \quad (26)$$

When the smaller star absorbs all the emitted radiation from the bigger star, we have  $\alpha_A = 0$ , and consequently, As a result, the solutions of Eqs (25) and (26) give

$$\rho_1 = \rho_2 = 1 \quad (27)$$

Therefore, we treat the reflective force of the smaller star as a perturbation, and can assume the solution of equations (25) and (26), to be

$$\rho_1 = 1 + \varepsilon_1 \text{ and } \rho_2 = 1 + \varepsilon_2 \quad (28)$$

Substituting Eqs (28) in Eqs (26), and applying binomial expansion while only retaining linear terms in  $\varepsilon_j (j = 1, 2)$ , we get

$$1 = \left[ 1 - \frac{v\alpha_A}{(1-v)k_1} \right] (1 - 3\varepsilon_1)$$

Solving and ignoring product of  $\varepsilon_1$  and  $\alpha_A$ , we at once get

$$\varepsilon_1 = -\frac{v\alpha_A}{3(1-v)k_1}$$

Similarly, we get

$$\varepsilon_2 = -\frac{\alpha_A}{3}$$

Hence, the solutions (28) become

$$\rho_1 = 1 - \frac{v\alpha_A}{3(1-v)k_1} \text{ and } \rho_2 = 1 - \frac{\alpha_A}{3} \quad (29)$$

Now, the exact coordinates of the TLPs are obtained from equations (19), and given by

$$\xi = \frac{1}{2} - v + \frac{\rho_2^2 - \rho_1^2}{2} \text{ and } \eta = \pm \left[ \frac{\rho_2^2 + \rho_1^2}{2} - \frac{1}{4} - \frac{(\rho_2^2 - \rho_1^2)^2}{4} \right]^{\frac{1}{2}} \quad (30)$$

Substituting Eqs (29) in (30), we at once get

$$\xi = \frac{1}{2} - v + \frac{1}{3} \left[ 1 - \frac{v}{k_1(1-v)} \right] \alpha_A, \quad \eta = \pm \frac{\sqrt{3}}{2} \left[ 1 - \frac{2}{9} \left\{ 1 + \frac{v}{k_1(1-v)} \right\} \alpha_A \right] \quad (31)$$

These two points given in Eqs (31) labelled as  $L_4(\xi, \eta)$  and  $L_5(\xi, -\eta)$ , and are called the TLPs by virtue of forming triangles with the primaries. The positions are defined by the mass and luminosity parameters of the stars and the reflective inclination of the smaller star.

Next, we compute the numerical estimates of the locations of the TLPs using the software *Mathematica* (Wolfram 2020). Further, the locations of the TLPs and ZVC are drawn to demonstrate the impact of the luminosity and mass variation parameters under effect of albedo.

For our numerical Illustrations, we consider a satellite-Proxima-Centauri system. The data for the binary Proxima-Centauri is taken from Yousuf & Kishor (2019) and given in Table 1:

**Table 1:** Numerical estimates for the Proxima Centauri system:

<b>System</b>	<b>Mass Parameter</b> ( $v$ )	<b>Reflective</b> <b>Coefficients</b> ( $\alpha_A$ )
<b>Proxima Centauri</b>	0.000031	0.0008

Now, in Table 2 we give the numerical estimates of the TLPs by computing equations (31), numerically for the Proxima Centauri configuration under mass variation and luminosity effects.

**Table 2:** Locations of the TLPs for the satellite-Proxima-Centauri system for  $0 < k_1 < 1$  and  $\alpha_A = 0.0008$

<b>S/N</b>	$k_1$	$\xi$	$\pm\eta$
<b>1</b>	0.000000001	-7.76722	-3.90704
<b>2</b>	0.00000001	- 0.32699	0.388580
<b>3</b>	0.0000001	0.417033	0.818142
<b>4</b>	0.000001	0.491435	0.861099
<b>5</b>	0.00001	0.498876	0.865394
<b>6</b>	0.0001	0.49962	0.865824
<b>7</b>	0.001	0.499694	0.865867
<b>8</b>	0.01	0.499702	0.865871
<b>9</b>	0.1	0.499702	0.865871
<b>10</b>	0.9999	0.499702	0.865871

In the RTBP with radiation, the luminosity affects the radiation pressure on particles. If  $k_1$  is the luminosity ratio, then when  $k_1$  is very small (0.00000001), it means the smaller star has extremely low reflective power, however when  $k_1$  is close to 1 (0.9999), both stars have nearly equal luminosity, meaning the smaller star has high reflective tendency. We observed from Table 2, that the values at the TLPs changes for  $0 < k_1 < 0.01$  but are the same when  $0.01 \leq k_1 < 1$ . The locations are plotted in Fig 2 (i-iii) for different values of  $k_1$  and a combined plots are given in Fig 2(iv) and Fig 3.

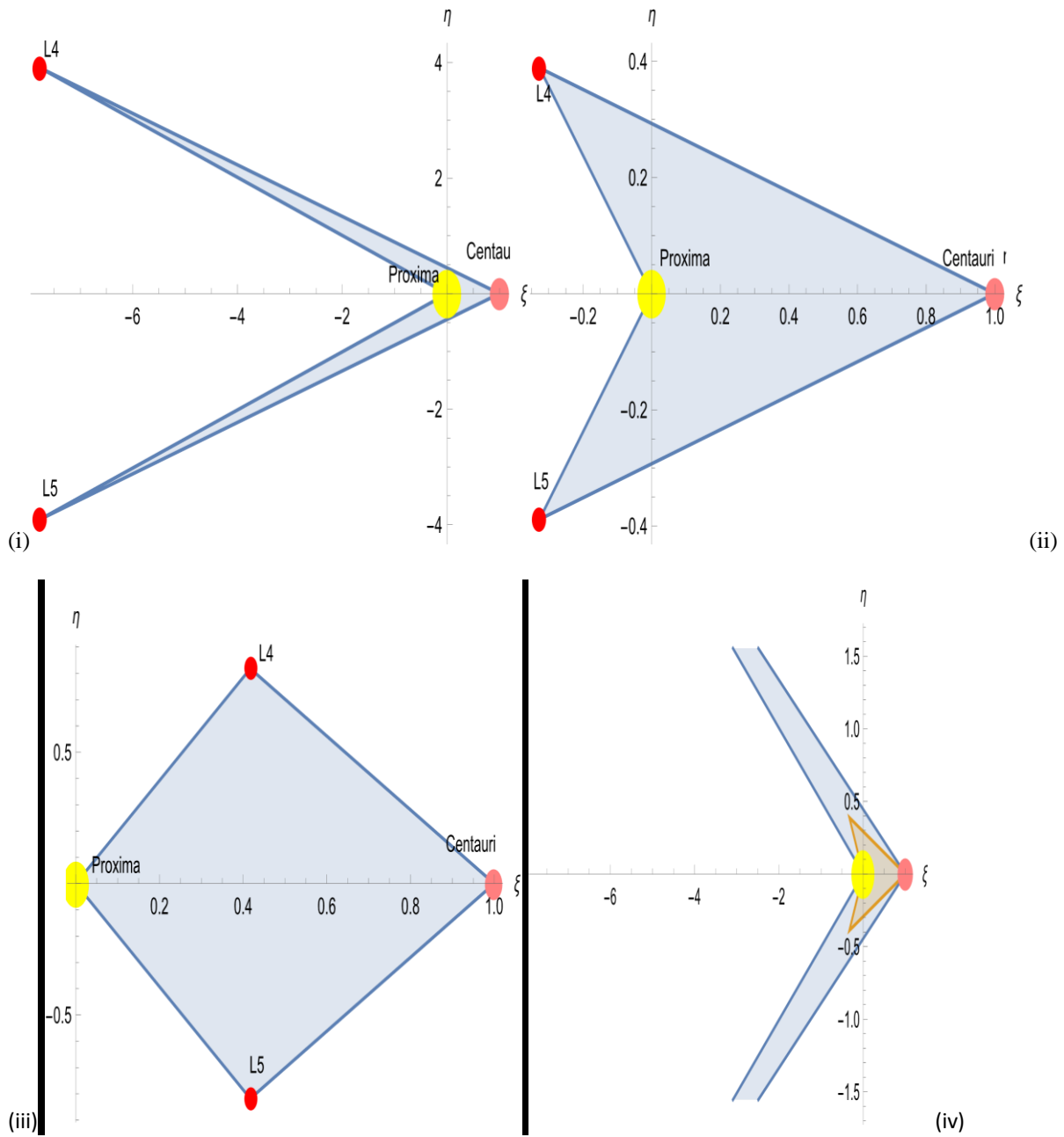


**Fig 2:** TLPs plotted for values given in (i) S/N 1, (ii) S/N 2 (iii) S/N 8 (iv) Combined plots of S/N 1 and 2

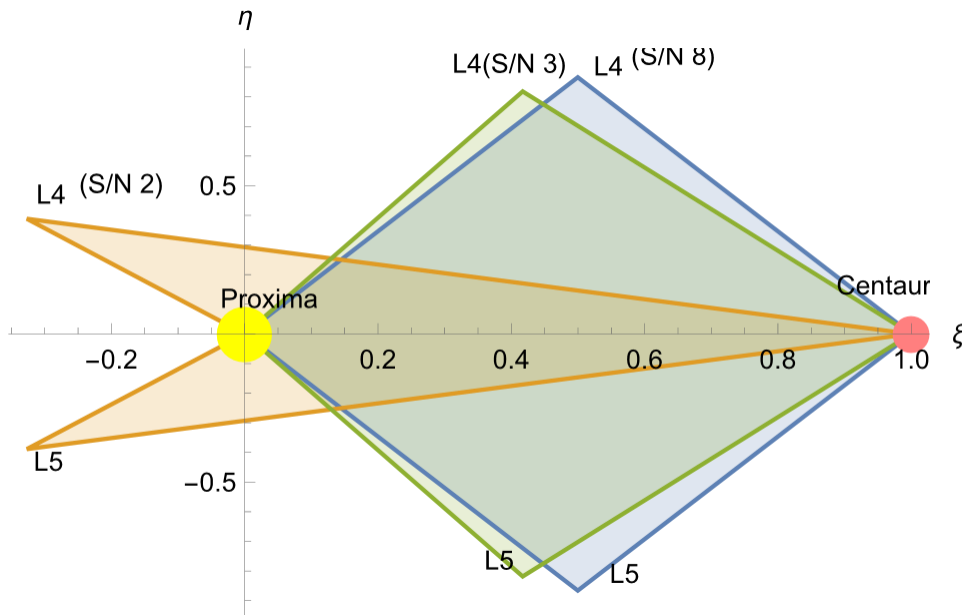


**Fig 3:** TLPs showing combined images plotted for values in S/N 2, 3 and 8  
 Fig 2 shows the TLP drawn for values computed in Table 2. The yellow sphere is the Proxima star while the pink represents the Centauri star. The red spots denote the locations of the TLPs. The first figure 1a, has been drawn using the values generated in serial number 1, while the second and third graphs have been drawn for values in serial number 2 and 8, respectively. The graphs shown in Fig 2(iv) and Fig 3 are the combined plots we have drawn to show the alterations in the locations of the TLPs due to the different values of the luminosity parameter of the stars.

Next, we obtain the TLPs of the time-variant system using the MT and are given by

$$x^{(i)} = \xi^{(i)}R(t), \quad y^{(i)} = \eta^{(i)}R(t), \quad (32)$$

where,  $\xi^{(i)}$ ,  $\eta^{(j)}$  ( $i = 4$ ) and ( $j = 4,5$ ) are the TLPs of the time-invariant system given in equations (31). The TLPs in this case are functions of time, and so the locations of the TLPs of time-variant system will always change with time.

Finally, using equation (16), we compute in Table 3, the values of the Jacobi constants  $J$  for diverse values of the mass variation factor  $\kappa$  of the stars and their luminosities  $k_1$ .

**Table 3:** Energy constants of the satellite around TLPs for  $0 < \kappa < \infty$ ,  $0 < k_1 < 1$  and  $\alpha_A = 0.0008$

$\kappa$	$k_1$	$J$
<b>0.000000001</b>	0.000001	$2.950 \times 10^{-10}$
	0.9999	$2.9999 \times 10^{-9}$
<b>0.00001</b>	0.000001	0.0000295016
	0.9999	0.0000299997
<b>0.01</b>	0.000001	0.0295016
	0.9999	0.0299997
<b>1</b>	0.000001	2.95016
	0.9999	2.99997
<b>2</b>	0.000001	5.90032
	0.9999	5.99994
<b>5</b>	0.000001	14.7508
	0.9999	14.9998
<b>10</b>	0.000001	29.5016
	0.9999	29.9998

0.9999

29.9997

The ZVCs around the TLPs are drawn for different values of the Jacobi constants which have been computed in Table 3. Fig 4-5 shows the ZVC of the satellite in the gravitational domain of the binary Proxima Centauri. The purple region are regions of allowed motion of the satellite, while the red region shows regions that the satellite is forbidden to move to. It is noted that for very small values of the Jacobi constants, the regions are all shown in the purple color as seen in Figures 3, and signifies that the satellite can roam freely around the TLPs, the binary and even beyond. This means that for low Jacobi constant the satellite has very high kinetic energy enough to make it escape into space. However, as the sum of the masses of the stars double, red region begins to show while the purple region begins to shrink, as seen in Figures 5.

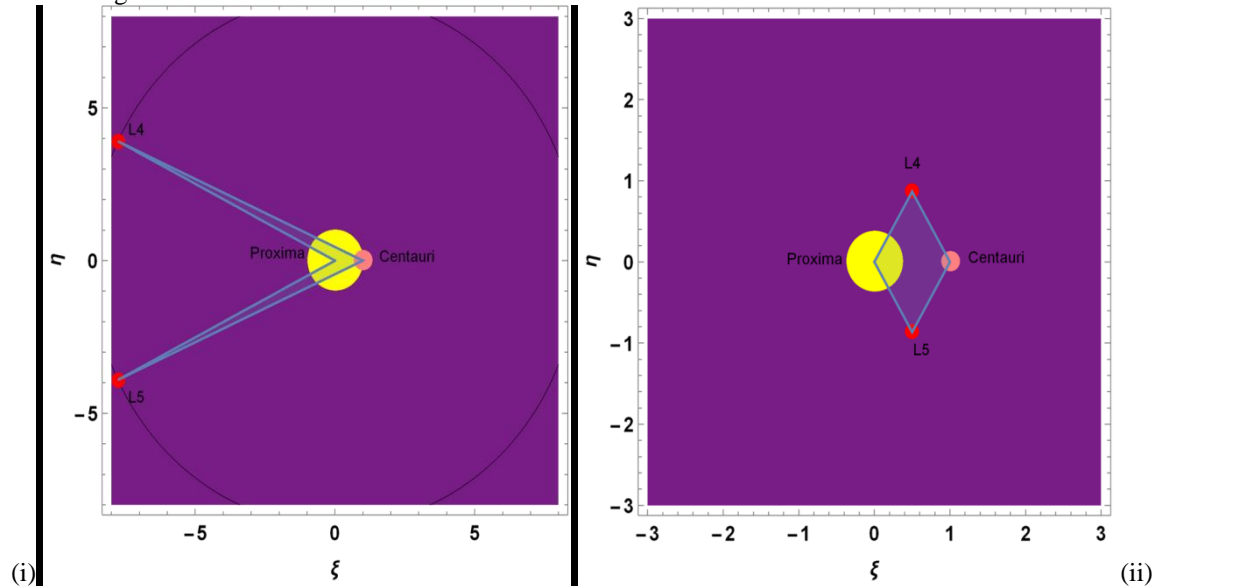
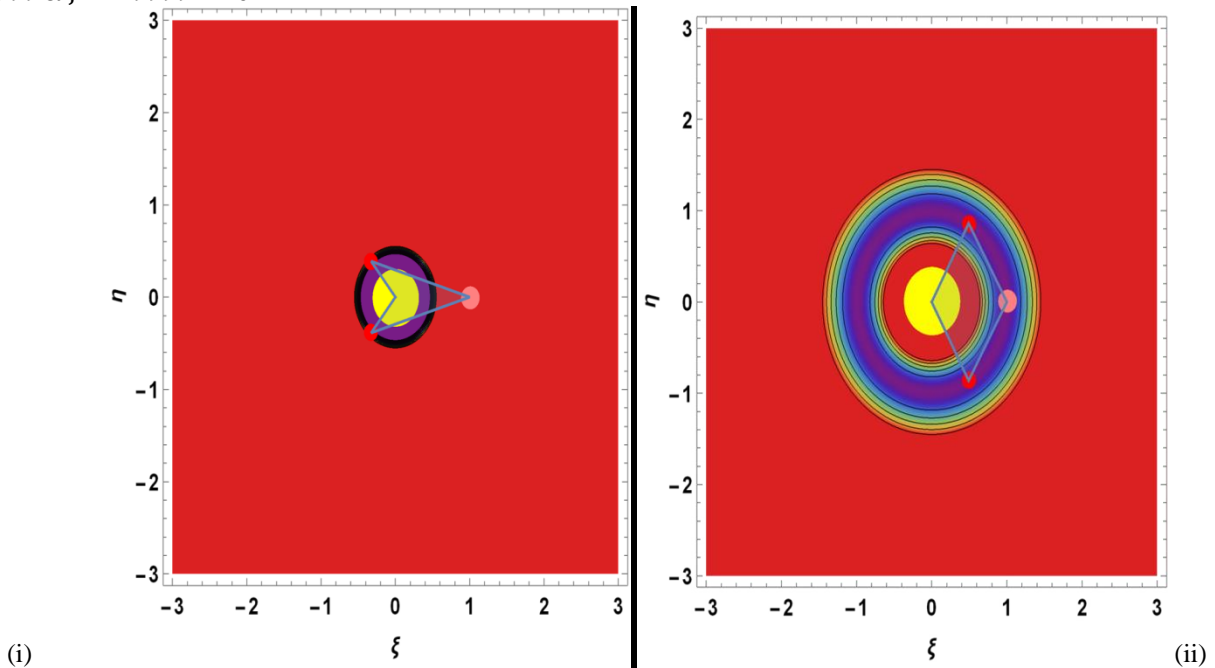


Fig 4: TLPs and ZVC for  $\kappa = 0.000000001$  when (i)  $k_1 = 0.000000001$ , &  $J = 7.012 \times 10^{-9}$  (ii)  $k_1 = 0.9999$  &  $J = 2.9999 \times 10^{-9}$



**Fig 5:** TLPs and ZVC for  $\kappa = 2$  when (i)  $k_1 = 0.000000001$ , &  $J = -11.1416$  (ii)  $k_1 = 0.9999$  &  $J = 5.99994$

### Discussion

The paper investigated the effects of the reflective and luminosity parameters of Proxima Centauri on locations and ZVCs of a satellite around the TLPs of the photo gravitational RTBP with capricious masses. The problem is photogravitational because the stars are luminous with their luminosities and masses varying in obedience to the UML while motion of both stars is governed by the GMP. Further, the larger star is a radiation emitter while the companion star has a reflective tendency.

We implemented the dynamical equations of Singh & Leke (2010) with the deviation that the second primary not only emits radiation but also reflects incoming radiation from the bigger star. These equations are different from those of those of Luk'yanov (1989), Bekov (1988), Singh & Leke (2012,2013), Leke & Singh (2023), Leke et al. (2024,2025) and Veronica et al. (2025) due to the photogravitational assumptions. However, they can all be recovered from our dynamical equations of motion. If we set  $q_1 = q_A = 1$ .

Next, the time-variant dynamical system was transformed to time-invariant equations and subsequently, the locations of the TLPs were calculated using the perturbation method. The points are defined by the luminosity, reflective behavior and the mass parameter of the stars. The TLPs are different from those obtained in Bekov (1988), Luk'yanov (1989), Singh & Leke (2010, 2012, 2013), Leke et al. (2024) and Veronica et al. (2025). The time-variant TLPs differ from those of the time-invariant equations by as function of time  $t$ .

We performed numerical illustrations to compute TLPs numerically and draw the locations. These locations are seen to shift under luminosity and reflective behaviors of the stars. Finally, the ZVC are explored for different values of the Jacobi constants which are a consequent of the luminosities and sum of the masses of the stars. It is observed that the reflective behaviour of the smaller star and the sum of the masses of the stars alters the topology of the ZVCs. Also, with regards to the impact of the luminosity parameter, it is observed that for some very small values of the sum of the stars the Jacobi constants are negative when the luminosity parameter is approaching zero, and the satellite has high kinetic energy to travel to any point and can escape from the vicinity of the TLPs

### Conclusion

This paper explored impact of luminosity parameter of Proxima Centauri on locations of TLPs of the photogravitational R3BP with capricious masses. In this study, the positions of a satellite in the gravitational domain of a larger star emitting radiation pressure whose companion star has reflective tendency, is located. The masses and luminosities of the stars are assumed to change with time in obedience with the UML and their movements maintained by the GMP. We formulated the time-variant dynamical equations and transform them to the time-invariant system with constant coefficients with the help of the MT, the UML, the particular solutions of the GMP and a transformation that represents the variable luminosities of the star. Thereafter, we calculated the locations of the TLPs for both systems of equations and it is seen that the later depends on the mass, luminosity and albedo parameters while former depends additionally within frame of variable mass.

### References

- Bekov, A. A. (1988). Libration points of the restricted problem of Three Bodies with Variable mass. *Soviet Astron. J.*, 33, 92-95
- Cyiril-Okeme, V., Leke, O., & Gyegwe J. (2025). Impacts of variable mass disk on region and stability of motion around triangular equilibrium points of the R3BP with variable mass binary MAXI J1659-152 and Kepler-16. *New Astronomy*. 121, 1024567
- Gao, F., & Wang, Y. (2020). Approximate analytical periodic solutions to the restricted three- body problem with perturbation, oblateness, radiation and varying mass. *Universe*, 6, 110

- Idrisi M.J., & Ullah M.S. (2018). Non-collinear libration in the ER3BP under albedo effects and oblateness. *J. Astrophys Astronomy*. 39, 28
- Idrisi, M. J., & Ullah, M. S. (2021). Out-of-plane equilibrium points in the elliptic restricted three-body problem under albedo effect. *New Astronomy*. 89, 101629.
- Idrisi, M.J. (2017). A study of libration points in CR3BP under albedo effect. *Int. J. of Adv. Astron.*, 5, 1-6.
- Jat, R.M. & Kishor, R. (2025). Impact of dark matter halo and albedo effect on the out-of-plane motion in the generalized photogravitational RTBP. *Physics of the Dark Universe*, 48, 101940
- Leke, O., & Akpii, B. (2025). Existence and stability of the collinear equilibrium points of the photogravitational restricted three body problem with variable masses and charges *African Journal of Mathematics, Statistics and Actuarial Science (AJMSAS)*, Vol. 1,83-112
- Leke, O., & Mmaju, C. (2023). Zero Velocity Curves of a Dust Grain Around Equilibrium Points Under Effects of Radiation, Perturbations and Variable Kruger 60. *Physics. Astronomy. International Journal* 7, 280-285
- Leke, O., & Orum, S. A. (2024). Motion and zero velocity curves of a dust grain around collinear libration points for the binary IRAS 11472-0800 and G29-38 with a triaxial star and variable masses. *New Astronomy*. 108, 102177
- Leke, O., & Singh, J. (2023). Out-of-plane equilibrium points of extra-solar planets in the central binaries PSR B1620-26 and Kepler-16 with cluster of material points and variable masses. *New Astronomy*. 99, 101958
- Leke, O., Cyril-Okeme, V. & Orum, S.A. (2024). Impact of triaxiality and mass variations on motion around triangular equilibrium points of the restricted three-body problem, *Astron. Reports*, 68,1117-1141
- Leke, O., Cyril-Okeme, V., Stephen, S. & Gyegwe, J., (2025a). Investigation of motion around out-of-plane points in the restricted three-body problem with variable shape and masses. *New Astronomy*. 114, 102311
- Leke, O., Kwaghnzua B, & Ashezua, T. (2025b). Divulging the Combined Effects of Radiation, Perturbations and Mass Variations on Motion around Axial Equilibrium Points of the Robe's R3BP. *Global Journal of Chemistry, Biology and Physics* 10 (4), 1-15
- Luk'yanov, L. G. (1989). Particular solutions in the restricted problem of three bodies with variable masses. *Astron. J. of Academy of Sciences of USSR*, 66, 180-187
- Putra, L.B., Nurul Huda, I. & Ramadhan, H. S., et al., (2024). Effects of variable mass, disk-like structure, and radiation pressure on the dynamics of circular restricted three-body problem, *Romanian Astron. J.* 1-2.03
- Singh, J., & Leke, O. (2012). Equilibrium points and stability in the restricted three-body problem with oblateness and variable masses. *Astrophys. Space Sci.*, 340: 27-41.
- Singh, J., & Leke, O. (2013). Effects of oblateness, perturbations, radiation and varying masses on the stability of equilibrium points in the restricted three-body problem. *Astrophys. Space Sci.* 344: 51-61.
- Singh, J., & Leke, O. (2010). Stability of the photogravitational restricted three-body problem with variable masses. *Astrophys. Space Sc*, 326, 305- 314.
- Szebehely, V.G. (1967). *Theory of Orbits*. Academic Press, New York.
- Wolfram, S.: (2020). *The Mathematica Book*. 5<sup>th</sup> Edition. Wolfram Media, Champaign
- Yadav, A.K., Kushvah, B.S., & Dolas, U. (2021). Controlling the libration point orbits for CRTBP with non-ideal solar sail and albedo effect. *Chaos, Solitons & Fractals*, 152, 111387
- Yousuf, S., & Kishor, R. (2019). Effects of albedo and disc on the zero velocity curves and linear stability of equilibrium points in the generalized restricted three-body problem. *Mon. N. Royal Astron. Soc.*, 488, 1894-1907.